

# dots.ocr: Multilingual Document Layout Parsing in a Single Vision-Language Model

Yumeng Li, Guang Yang, Hao Liu, Bowen Wang, Colin Zhang  
hi lab, Xiaohongshu Inc

 <https://github.com/rednote-hilab/dots.ocr>

## Abstract

*Document Layout Parsing serves as a critical gateway for Artificial Intelligence (AI) to access and interpret the world’s vast stores of structured knowledge. This process, which encompasses layout detection, text recognition, and relational understanding, is particularly crucial for empowering next-generation Vision-Language Models. Current methods, however, rely on fragmented, multi-stage pipelines that suffer from error propagation and fail to leverage the synergies of joint training. In this paper, we introduce dots.ocr, a single Vision-Language Model that, for the first time, demonstrates the advantages of jointly learning three core tasks within a unified, end-to-end framework. This is made possible by a highly scalable data engine that synthesizes a vast multilingual corpus, empowering the model to deliver robust performance across a wide array of tasks, encompassing diverse languages, layouts, and domains. The efficacy of our unified paradigm is validated by state-of-the-art performance on the comprehensive OmniDocBench. Furthermore, to catalyze research in global document intelligence, we introduce XDocParse, a challenging new benchmark spanning 126 languages. On this benchmark, dots.ocr achieves state-of-the-art performance, delivering an approximately 10% relative improvement and demonstrating strong multilingual capability.*

## 1. Introduction

Document Layout Parsing [23, 30, 38, 48] is a fundamental capability for Artificial Intelligence to comprehend the vast repository of structured human knowledge. It not only powers downstream applications like intelligent process automation but also acts as a crucial data engine for training next-generation Vision-Language Model (VLM) [28, 37]. Despite its foundational importance, parsing documents at scale, with high fidelity, and across the world’s diverse spectrum of languages, layouts, and domains remains a formidable challenge.

The first challenge is architectural. Comprehensive document parsing requires mastering a trinity of interconnected sub-tasks: (1) Layout Detection [14, 51], to identify the spatial boundaries of elements like paragraphs and figures; (2) Content Recognition [10, 35], to extract the text and symbols within them; and (3) Relational Understanding [17, 36, 45], to infer logical connections such as reading order. However, the dominant paradigm [7, 42] addresses these through fragmented, multi-stage pipelines, treating them as isolated steps. This separation, while modular, introduces two key limitations: it is prone to cascading errors, where mistakes in an early stage impairs subsequent ones, and fails to capitalize on the powerful synergies between tasks [50].

A second major challenge concerns data and scale [24, 52]. Progress in document parsing has been overwhelmingly Anglo-centric, leaving a vast majority of the world’s languages critically underserved [49]. The root cause is the prohibitive cost of curating diverse, large-scale annotated datasets. This data bottleneck, in turn, creates a difficult trade-off between cost and performance: while pipeline systems are more data-efficient, they are complex to maintain and often hit a performance ceiling. Conversely, emerging end-to-end models [34, 44] promise higher performance but demand prohibitive computational resources, hindering their scalability.

To overcome these barriers, we introduce dots.ocr, a single, unified framework designed to achieve high performance, multilingual capability, and scalability. On the one hand, our unified VLM architecture is the first to demonstrate both the viability and superiority of jointly learning layout detection, content recognition, and relational understanding within a single end-to-end pass. On the other hand, to tackle the aforementioned data bottleneck, we built a highly scalable data engine. By synthesizing a vast corpus of high-quality multilingual training data, it alleviates the need for expensive manual annotation and enables robust generalization capabilities.

The effectiveness of our unified paradigm is rigorously demonstrated on the comprehensive OmniDocBench [29],

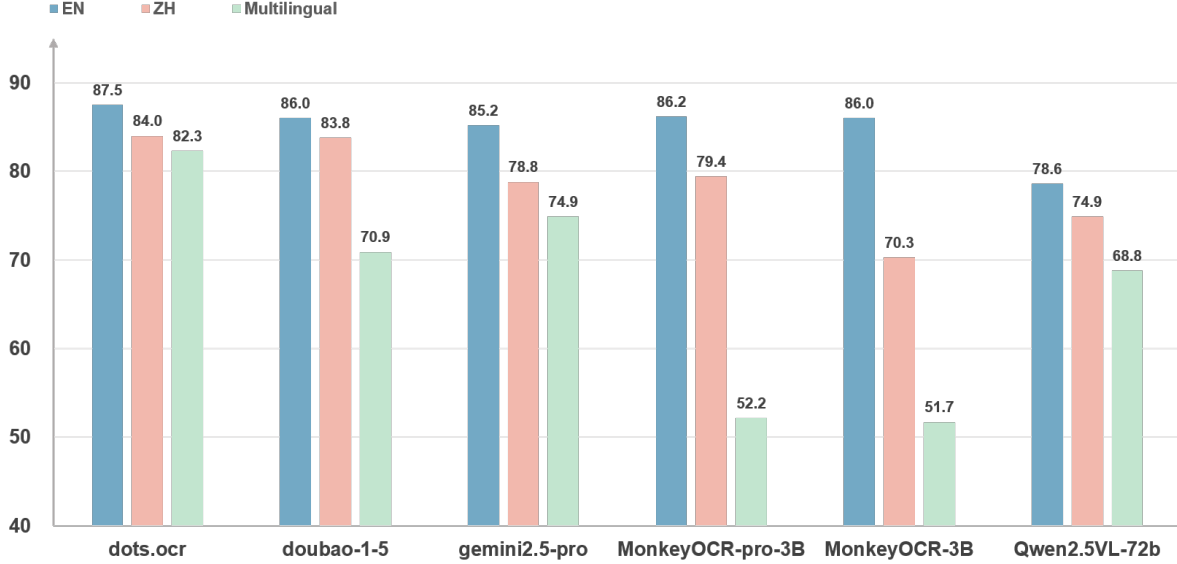


Figure 1. **Performance comparison of dots.ocr with other state-of-the-art methods.** We evaluate performance on the comprehensive OmniDocBench[29] benchmark for English (EN) and Chinese (ZH), and on our newly proposed XDocParse benchmark for large-scale multilingual evaluation (Multilingual). **dots.ocr** consistently outperforms all competing methods across all three settings, demonstrating its superior capability.

where we achieve new state-of-the-art scores of 87.5 (EN) and 84.0 (CH). To further advance research in global document intelligence, we introduce XDocParse—a challenging new benchmark covering 126 languages. On this testbed, dots.ocr sets a robust new baseline, surpassing the previous best competitor by an impressive margin of +7.4 points, and showcasing its unparalleled multilingual capabilities.

In summary, our main contributions are as follows:

- **A Unified Architecture with State-of-the-Art Performance.** We introduce dots.ocr, a single VLM architecture that is the first to demonstrate both the viability and superiority of jointly learning layout detection, content recognition, and relational understanding. This holistic design, validated by extensive ablation studies showing its superiority over pipelined approaches, enables the model to deliver exceptional performance on OmniDocBench [29].
- **A Scalable Multilingual Data Engine.** We designed a highly scalable data engine that powers our unified model. It systematically overcomes the data bottleneck by synthesizing a vast, diverse corpus, directly empowering the model with robust generalization capabilities across various languages, layouts, and document types. Furthermore, The critical role of this data engine is substantiated by extensive ablation studies.
- **A New Large-Scale Multilingual Benchmark.** To spur research in global document intelligence, we introduce and will release XDocParse, a challenging benchmark spanning 126 languages. We establish a strong new baseline with dots.ocr, which significantly outperforms all ex-

isting methods on this demanding testbed.

## 2. Related work

### 2.1. General VLMs for Document Parsing

The rapid advancement of powerful general Vision-Language Models (VLMs) like GPT-4o [15], Gemini 2.5 Pro [6], and Qwen2.5-VL [2] has opened new avenues for high-level document understanding, such as summarization and question answering. However, their suitability for fine-grained, large-scale document parsing is limited by two fundamental challenges. First, as recent studies show [43], these generalist models lack the architectural priors for structured analysis, often struggling with precise layout localization and dense text recognition. Second, their prohibitive computational cost and high latency render them impractical for processing the vast volumes of documents required in data pipelines. This fundamental mismatch, both in architecture and efficiency, necessitates the development of specialized VLMs explicitly designed for document parsing.

### 2.2. Specialized VLMs for Document Parsing

In response, a distinct line of research on specialized Document VLMs [32, 41] has emerged. The journey began with OCR-free pioneers like Donut [16] and Nougat [3], which focused primarily on text recognition. More recently, the ambition has grown to unify the full spectrum of document parsing tasks, but current approaches remain fragmented in

different ways. For instance, MonkeyOCR [19] relies on an explicit multi-stage pipeline, separately processing structure and content. Other models achieve a semblance of unification by omitting key tasks entirely. OlmOCR [34], for example, only parses content from given regions without layout detection. And Dolphin [11], which uses a single model, internally employs a two-stage “analyze-then-parse” process. This staged design leads to suboptimal performance, particularly in complex tasks like reading order inference, revealing that a truly synergistic, unified paradigm has not yet been achieved. In contrast, dots.ocr achieves synergistic joint learning by modeling the interdependences between layout, content, and relations within a single, end-to-end generative process, which is a capability previously unattainable with staged approaches.

### 2.3. Datasets for Multilingual Document parsing

Beyond architectural design, a more fundamental challenge limiting the generalization of these specialized models is the severe scarcity of multilingual data for both training and evaluation [47]. The vast majority of influential training datasets, such as M6Doc [5], D4LA [8], and DocLayNet [33], are English-centric. Other resources, like CDLA [18], typically cover only one other major language. This lack of diverse training data hinders the development of truly global models [1]. The problem is mirrored in the evaluation landscape: leading benchmarks like OmniDocBench [29] also primarily focus on high-resource languages, making it impossible to assess true multilingual robustness. This dual scarcity in training and evaluation underscores the urgent need to actively generate diverse multilingual data and establish a comprehensive benchmark to fairly assess true cross-lingual generalization.

## 3. Method

Our approach, dots.ocr, is designed to perform end-to-end document parsing by unifying three core tasks within a single Vision-Language Model: layout detection, text recognition, and relational understanding, which we operationalize through the task of reading order generation. Realizing this unification requires fundamental innovations on two fronts, which we deliver through: (1) a **specialized training paradigm**, encompassing specific architectural choices and training strategies tailored for unified OCR tasks, and (2) a **holistic data engine** that generates the massive, multi-dimensionally diverse corpus necessary for robust training.

We now detail our approach. We begin by defining the unified task formulation that serves as the foundation for our method (Sec. 3.1). We then present the specifics of our model architecture and training process, detailing how we adapt a VLM for this unified task (Sec. 3.2). Finally, we describe our holistic data engine, the mechanism responsible for generating the diverse, large-scale corpus that makes

our unified training paradigm feasible (Sec. 3.3).

### 3.1. Unified Task Formulation

We formulate multilingual document parsing as a single, end-to-end autoregressive generation task. This unified formulation compels the model to learn the intricate interplay between an element’s visual layout, textual content, and semantic role.

Given a document image  $\mathbf{I}$ , the model outputs a structured sequence  $\mathbf{S}$ , where each entry corresponds to a semantic content block. Formally, the output sequence is:

$$\mathbf{S} = [(\mathcal{B}_1, c_1, t_1), \dots, (\mathcal{B}_K, c_K, t_K)] \quad (1)$$

where  $K$  denotes the number of detected blocks. Each tuple  $(\mathcal{B}_k, c_k, t_k)$  represents the  $k$ -th block, with  $\mathcal{B}_k = (x_{k,1}, y_{k,1}, x_{k,2}, y_{k,2})$  as the bounding box coordinates,  $c_k \in \mathcal{C}$  as the block category (e.g., title, header, table, figure), and  $t_k$  as the recognized textual content. For unstructured blocks,  $t_k$  is plain text; for structured regions such as tables,  $t_k$  is encoded in Latex format to capture detailed layout and hierarchy.

Crucially, the sequence  $\mathbf{S}$  is generated in an order that **aligns with human reading progression**. This task formulation compels the model to not only parse content but also to comprehend the document’s logical flow, thus unifying layout detection, text recognition, and high-level relational understanding in a single pass.

### 3.2. Model Architecture for Unified Parsing

To accomplish our unified task, we adopt a ViT-LLM architecture. This design is inspired by recent advances in large vision-language models such as Qwen2-VL [2], but incorporates critical modifications to both the vision encoder and the language decoder, tailored for unified document parsing.

**Vision Encoder:** We employ a 1.2B parameter Vision Encoder (VE) trained entirely from scratch, a deliberate departure from fine-tuning pre-trained, image-centric encoders. This from-scratch approach allows us to specialize its feature representation for document intelligence from the ground up. Architecturally, we design the VE to handle native high-resolution inputs of up to 11 million pixels [9], enabling it to process dense documents. The training objective is multi-faceted, compelling the encoder to jointly master both fine-grained visual details for text recognition and high-level layout structures for relational understanding. This specialized, high-resolution VE provides a powerful foundation for the unified parsing task.

**Language Model Decoder:** For the decoder, we select the Qwen2.5-1.5B base model as our foundation, a choice guided by the need to balance computational efficiency with the expressive capacity required for complex relational understanding. With modifications including tied word embeddings, the final decoder comprises 1.7B parameters.

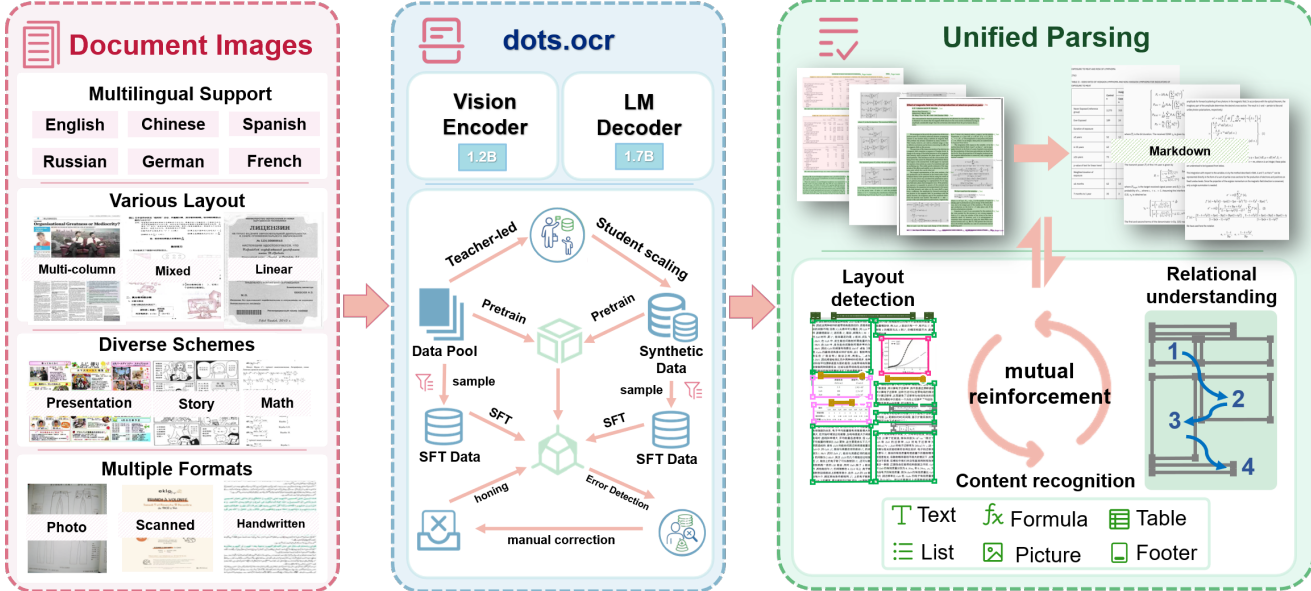


Figure 2. **Overview of the dots.ocr.** (**Left**) Our system processes a diverse spectrum of document images, varying in language, layout, and format. (**Center**) At its core is a Vision-Language Model (VLM) whose training is powered by our holistic Data Engine. (**Right**) The model jointly performs three mutually reinforcing tasks—layout detection, content recognition, and relational understanding.

Crucially, initializing from the base model is a choice dictated by our large-scale pre-training paradigm. A base model provides the neutral, adaptable foundation essential for our training, which aims to teach the model the non-natural syntax and complex structures of diverse documents from the ground up, rather than adapting a model already specialized for conversational tasks.

### 3.3. Data Engine for Unified Multilingual Parsing

Training a unified model for multilingual document parsing imposes extreme demands on the training data. It requires a corpus that is not only massive in scale but also exceptionally diverse across several critical axes such as linguistic breadth, layout diversity, topical variety and so on. Since no existing dataset meets these stringent requirements, we engineered a novel, three-stage Data Engine to systematically construct our training corpus.

**Stage 1: Bootstrapping a Multilingual Synthesis Engine.** The foundational challenge is the near-total absence of structured, labeled document data outside of high-resource languages. To overcome this, our first stage bootstraps a scalable synthesis engine via teacher-student distillation.

**(1) Teacher-Led Structured Generation.** We employ a powerful proprietary VLM (Qwen2.5-VL-72B[2]) as a “teacher” and task it with a structured re-rendering task: given a labeled English document and its structural representation, the teacher is prompted to generate a semantically equivalent document in a target language while preserving

the original layout logic. This output is then rendered into a new image, creating a high-quality, parallel seed document.

**(2) Distilling to a Scalable Student.** This process, while high-quality, is too slow and expensive for mass production. Therefore, we use the generated multilingual seed corpus to fine-tune a smaller, more efficient Qwen2.5-VL-7B[2] model. This “student” model distills the core, structure-aware, cross-lingual generation capability of its teacher. The key outcome of this stage is not the data itself, but the creation of a specialized and highly scalable auto-labeling engine for the next stage.

**Stage 2: Strategically Curated Corpus for Large-Scale Pre-training.** Leveraging our synthesis engine from Stage 1, we generate a massive pre-training corpus, prioritizing strategic curation over raw scale. We perform deep stratified sampling on our internal data, using heuristics to profile documents by layout complexity (e.g., column count, table density), linguistic rarity, and domain. To combat the inherent biases in large datasets, we purposefully over-sample from under-represented strata, such as complex multi-language tables and documents from niche scientific domains. Our 7B student model then auto-labels this high-diversity, curated pool, transforming millions of raw PDFs into a structured pre-training dataset. Ultimately, this curation-first approach ensures pre-training is not just large-scale, but high-impact—endowing the model with a deep, generalizable understanding of document structure essential for real-world parsing.

**Stage 3: Honing the Model via Targeted Correction.**

Training on the massive corpus from the first two stages equips our base model with a broad, foundational understanding. However, this latent knowledge must be precisely honed to perform the unified parsing task with high fidelity. The objective of this final stage is therefore to align the model’s emergent abilities, ensuring it can synergistically execute the core tasks of layout detection, text recognition, and relational understanding within a single forward pass.

This alignment is achieved via a systematic Human-in-the-Loop (HITL) error correction cycle, initiated by using the pre-trained model to perform inference on our diverse document pool. These initial predictions then undergo a programmatic audit, where a powerful VLM (Qwen2.5-VL-7B-Instruct [2]), acting as an oracle, diagnoses a full spectrum of failure modes, identifying straightforward issues like localization inaccuracies and content or type errors, while confirming more subtle omissions and hallucinations through the examination of masked or cropped document regions.

These high-confidence, verified error cases are then routed to human annotators for efficient correction. The resulting high-signal dataset, now comprising over 15,000 samples rich in the model’s specific weaknesses, provides a powerful, focused gradient that transforms the model from a broadly capable generalist into a precise and reliable parsing expert.

## 4. Experiments

### 4.1. Experimental Setting

**Implementation Details.** Our model, dots.ocr, consists of a 1.2B-parameter Vision Encoder (VE) and a 1.7B-parameter Language Model Decoder. It is initialized from a powerful, OCR-specialized base model (Sec. 3.2) and then supervised finetuned (SFT) on approximately 300k diverse samples. For finetuning, we used the AdamW optimizer [21] with a peak learning rate of 5e-5 and a cosine decay schedule.

**Evaluation Benchmarks and Metrics.** We conduct our primary end-to-end evaluation on OmniDocBench [29], following its official protocol. We report OverallEdit, along with its component-specific scores. Supporting results on olmOCR-Bench [34] are provided in Appendix 7, and our model’s extensive multilingual capabilities are thoroughly examined in Sec. 4.3.

### 4.2. Main Results on OmniDocBench

Table 1 presents a comprehensive comparison on the OmniDocBench [29]. The results unequivocally demonstrate the superiority of our proposed model, dots.ocr, which achieves state-of-the-art performance across nearly all key metrics in both English and Chinese.

**Overall Performance.** dots.ocr sets a new state of the art, achieving an OverallEdit score of 0.125 in English and 0.160 in Chinese. This represents a significant improvement over the best-performing baselines, including specialized expert models like MonkeyOCR-pro-3B [19] (0.138 EN) and powerful generalist VLMs like doubaos-1-5 [13] (0.162 ZH). This holistic metric, which encapsulates all aspects of document parsing, highlights the profound benefits of our unified end-to-end learning paradigm. By jointly optimizing for detection, recognition, and structural understanding, dots.ocr effectively mitigates the error propagation inherent in pipeline-based tools and surpasses the capabilities of even the most powerful, yet fragmented, approaches.

**Component-level Dominance.** The superiority of dots.ocr is not just holistic but also evident at the component level, where it demonstrates excellence in both text recognition and structural understanding. On the one hand, it achieves a remarkable TextEdit score of 0.032 (EN) and 0.066 (ZH), significantly outperforming all other methods. This demonstrates the power of our data engine and the advantage of contextual awareness in a unified architecture. On the other hand, it excels in structural tasks, evidenced by its leading performance in TableTEDS (88.6 EN) and near-best in Chinese (89.0), as well as TableEdit. Furthermore, its state-of-the-art Reading Order Edit scores (0.040 EN, 0.067 ZH) demonstrate a superior understanding of the natural document flow, a crucial and often overlooked aspect of complex relational understanding.

In summary, the results on OmniDocBench [29] robustly validate our approach. dots.ocr not only sets a new state-of-the-art but also by demonstrating the clear advantages of a truly unified, end-to-end model powered by a strategic data engine.

### 4.3. Multilingual Evaluation on XDocParse

**XDocParse benchmark.** Existing document parsing benchmarks are predominantly composed of English and Chinese documents, failing to provide a true measure of a model’s multilingual generalization capabilities. To address this critical gap, we introduce XDocParse, a new, comprehensive evaluation suite constructed from real-world documents spanning 126 languages. This benchmark serves as a challenging testbed to rigorously assess the end-to-end parsing performance of models across a vast and diverse linguistic landscape.

**Multilingual Performance.** We compare dots.ocr with a range of strong baselines, including specialized models (MonkeyOCR-3B [19]) and powerful proprietary VLMs (doubaos series [13], Gemini-2.5-Pro [6]). The results on our XDocParse benchmark are presented in Table 2. The results unequivocally demonstrate the superiority of our approach. dots.ocr establishes a new state-of-the-art across every single metric. Notably, in the crucial Overall Edit distance,

Table 1. State-of-the-art comparison on the **OmniDocBench** benchmark.

Model Type	Methods	OverallEdit ↓		TextEdit ↓		FormulaEdit ↓		TableTEDS ↑		TableEdit ↓		Reading Order Edit ↓	
		EN	ZH	EN	ZH	EN	ZH	EN	ZH	EN	ZH	EN	ZH
Pipeline Tools	MinerU [42]	0.150	0.357	0.061	0.215	0.278	0.577	78.6	62.1	0.180	0.344	0.079	0.292
	Marker [31]	0.336	0.556	0.080	0.315	0.530	0.883	67.6	49.2	0.619	0.685	0.114	0.340
	Mathpix [25]	0.191	0.365	0.105	0.384	0.306	0.454	77.0	67.1	0.243	0.320	0.108	0.304
	Doccling [20]	0.589	0.909	0.416	0.987	0.999	1.000	61.3	25.0	0.627	0.810	0.313	0.837
	Pix2Text [4]	0.320	0.528	0.138	0.356	0.276	0.611	73.6	66.2	0.584	0.645	0.281	0.499
	Unstructured [40]	0.586	0.716	0.198	0.481	0.999	1.000	0.0	0.06	1.000	0.998	0.145	0.387
	OpenParse [12]	0.646	0.814	0.681	0.974	0.996	1.000	64.8	27.5	0.284	0.639	0.595	0.641
Expert VLMs	PPStruct-V3 [7]	0.145	0.206	0.058	0.088	0.295	0.535	-	-	0.159	0.109	0.069	0.091
	GOT-OCR [46]	0.287	0.411	0.189	0.315	0.360	0.528	53.2	47.2	0.459	0.520	0.141	0.280
	Nougat [3]	0.452	0.973	0.365	0.998	0.488	0.941	39.9	0.0	0.572	1.000	0.382	0.954
	Mistral OCR [39]	0.268	0.439	0.072	0.325	0.318	0.495	75.8	63.6	0.600	0.650	0.083	0.284
	OLMOCR-slang [34]	0.326	0.469	0.097	0.293	0.455	0.655	68.1	61.3	0.608	0.652	0.145	0.277
	SmolDocling-256M [26]	0.493	0.816	0.262	0.838	0.753	0.997	44.9	16.5	0.729	0.907	0.227	0.522
	Dolphin [11]	0.206	0.306	0.107	0.197	0.447	0.580	77.3	67.2	0.180	0.285	0.091	0.162
	MinerU 2 [42]	0.139	0.240	0.047	0.109	0.297	0.536	82.5	79.0	0.141	0.195	0.069	0.118
	OCRFlux [27]	0.195	0.281	0.064	0.183	0.379	0.613	71.6	81.3	0.253	0.139	0.086	0.187
	MonkeyOCR-pro-3B [19]	0.138	0.206	0.067	0.107	<b>0.246</b>	0.421	81.5	87.5	0.139	0.111	0.100	0.185
General VLMs	GPT4o [15]	0.233	0.399	0.144	0.409	0.425	0.606	72.0	62.9	0.234	0.329	0.128	0.251
	Qwen2-VL-72B [44]	0.252	0.327	0.096	0.218	0.404	0.487	76.8	76.4	0.387	0.408	0.119	0.193
	Qwen2.5-VL-72B [2]	0.214	0.261	0.092	0.180	0.315	0.434	82.9	83.9	0.341	0.262	0.106	0.168
	Gemini2.5-Pro [6]	0.148	0.212	0.055	0.168	0.356	0.439	85.8	86.4	0.130	0.119	0.049	0.121
	doubao-1-5 [13]	0.140	0.162	0.043	0.085	0.295	<b>0.384</b>	83.3	<b>89.3</b>	0.165	<b>0.085</b>	0.058	0.094
our model	<b>dots.ocr</b>	<b>0.125</b>	<b>0.160</b>	<b>0.032</b>	<b>0.066</b>	0.329	0.416	<b>88.6</b>	89.0	<b>0.099</b>	0.092	<b>0.040</b>	<b>0.067</b>

Table 2. End-to-end performance comparison on our **XDocParse** benchmark.

Methods	Overall Edit ↓	TextEdit ↓	Formula Edit ↓	Table TEDS ↑	Table Edit ↓	Reading Order Edit ↓
MonkeyOCR-3B	0.483	0.445	0.627	50.93	0.452	0.409
doubao-1-5-thinking-vision-pro-250428 [13]	0.291	0.226	0.440	71.20	0.260	0.238
doubao-1-6 [13]	0.299	0.270	0.417	71.00	0.258	0.253
Gemini-2.5-Pro [6]	0.251	0.163	0.402	77.10	0.236	0.202
<b>dots.ocr (ours)</b>	<b>0.177</b>	<b>0.075</b>	<b>0.297</b>	<b>79.20</b>	<b>0.186</b>	<b>0.152</b>

our model (0.177) achieves a 29.5% relative reduction in error compared to the next-best model, Gemini-2.5-Pro [6] (0.251). The improvement is even more dramatic in Text Edit distance, where dots.ocr (0.075) more than halves the error of Gemini-2.5-Pro [6] (0.163), showing a 54% relative reduction. This highlights the exceptional text recognition quality fostered by our unified training paradigm.

## 5. Ablation study

In this section, we conduct a series of extensive ablation studies to systematically dissect the contributions of our unified design and data-centric approach. We complement our quantitative results with qualitative examples in Appendix 9, which visually illustrate the key findings of our analyses.

Our experiments are designed to test three central hypotheses. First, we investigate **the synergy of joint task learning**, positing that the constituent tasks form a symbiotic triad, mutually reinforcing each other within the uni-

fied framework. Second, we aim to prove **the superiority of the unified paradigm** itself, hypothesizing that a jointly trained model develops a richer contextual representation that makes it a more powerful specialist than models trained on a single task from the outset. Finally, we examine **the efficacy of our data engine**, ablating key components of our multilingual synthesis strategy to quantify their impact on robust, cross-lingual generalization .

### 5.1. The Synergy of Joint Task Learning

**Experimental Setup.** Our synergy ablation relies on a controlled setup built upon a training dataset comprising 116K document images. From this collection, we generate four distinct training configurations, each built upon the same set of input images but supplied with a different set of target annotations.

- **M<sub>Det</sub>**, trained **without detection** targets to predict an ordered sequence of text.
- **M<sub>Rec</sub>**, trained **without recognition** targets to predict an ordered sequence of bounding boxes.

Table 3. **Ablation study on the synergy of joint task learning.** We evaluate model variants trained without specific sub-tasks to quantify their contribution.

Configuration	Overall Edit		Reading Order Edit		Detection (F1)
	EN	CH	EN	CH	
<b>Unified (ours)</b>	<b>0.142</b>	<b>0.201</b>	<b>0.043</b>	<b>0.086</b>	0.822
M <sub>Rec</sub>			N/A		<b>0.832</b>
M <sub>Det</sub>	0.143	0.211	0.058	0.108	N/A
M <sub>RO</sub> (horz)	0.236	0.254	0.379	0.262	0.827
M <sub>RO</sub> (vert)	0.214	0.316	0.315	0.544	0.825
M <sub>RO</sub> (rand)	0.324	0.362	0.726	0.658	0.738

- M<sub>RO</sub>, trained **without ground-truth reading order**, relying instead on heuristic sorting schemes: horizontal (*horz*), vertical (*vert*), or random (*rand*).

A separate model is trained for each configuration. To ensure a fair comparison, all models are trained for an identical number of epochs with the same hyperparameters and are subsequently evaluated on the comprehensive OmniDocBench [29].

**Evaluation Metric.** For text recognition and reading order, we follow the official OmniDocBench [29] protocols. However, for layout detection, we introduce a F1-score-based metric. This is because the standard mAP metric is ill-suited for autoregressive models, as it requires confidence scores they do not natively produce and is sensitive to annotation inconsistencies. Our F1-based approach is confidence-free and more robust to inconsistencies in annotation granularity, ensuring a fairer evaluation. Implementation details are in Appendix 8.

**Results and Analysis.** The results in Table 3 reveal a deep, synergistic interplay between the core tasks. Ablating a single task significantly impairs the performance of the remaining ones, providing clear quantitative evidence of their mutual dependence. We analyze these cross-task impacts in detail below:

**(1) Layout Detection as a Geometric Foundation.** As evidenced by our results, ablating the detection task (M<sub>Det</sub>) leads to a significant degradation in the model’s ability to predict reading order. The Reading Order Edit score deteriorates by 34.9% for English (from 0.043 to 0.058) and 25.6% for Chinese (from 0.086 to 0.108), accompanied by a slight increase in Overall Edit. This confirms that a precise spatial detection is a prerequisite for inferring the document’s logical flow. Without it, the model struggles to reconstruct a coherent text sequence from disembodied content.

**(2) Text Recognition as a Semantic Regularizer.** Text recognition imposes a powerful semantic constraint on the detection task. Counter-intuitively, ablating recognition (M<sub>Rec</sub>) results in a slight improvement in the detection

score (0.832 vs. 0.822). We posit this is not because recognition is irrelevant, but because it acts as a beneficial regularizer. In the unified model, the detection objective is not merely to find any box, but to find boxes conducive to recognition. This semantic-driven pressure guides the detector toward more legible text regions, ultimately benefiting the end-to-end goal, even at the cost of a marginal drop in the isolated detection metric.

### (3) Reading Order as a Structural-Semantic Bridge.

A coherent reading order signal is critical for bridging low-level vision with high-level structure. This is evident as we degrade the training sequence from heuristic sorting (vertical, horizontal) to random shuffling. Not only do the text and order metrics worsen, but the detection score also plummets from 0.827 to 0.738. This demonstrates that an incoherent sequence does more than just confuse the final output, it corrupts the model’s internal representation of the document layout. It suggests that in VLMs, fundamental visual perception is not learned in isolation but is deeply intertwined with structural and semantic understanding.

In summary, these ablation studies reveal that layout detection, text recognition, and relational understanding are not independent modules but a symbiotic triad. Within our unified VLM, each task provides crucial inductive biases that guide and regularize the others. This reciprocal reinforcement leads to a level of holistic and robust document comprehension that fragmented, multi-stage pipelines cannot achieve.

## 5.2. Superiority of the Unified Paradigm

**Experimental Setup.** Having established the synergy between tasks, we now aim to prove the inherent superiority of our unified paradigm itself. We hypothesize that the rich contextual understanding gained during joint training makes our model a more powerful **specialist**—outperforming models trained solely on a single task from the outset. To isolate this effect, we design an experiment to disentangle the benefits of unified training from unified inference. We compare three distinct configurations:

- U → U (**Unified** → **Unified**). Our full dots.ocr model, trained and evaluated on all tasks jointly. This represents our full end-to-end paradigm.
- U → S (**Unified** → **Specialist**). The same jointly-trained model, but evaluated on a single, specialized task at inference time. This isolates the benefit of unified training.
- S → S (**Specialist** → **Specialist**). A baseline model trained and evaluated on only a single, specialized task. This configuration represents the dominant paradigm of existing specialized methods.

**Results and Analysis.** Table 4 dissects the advantages of our unified paradigm by comparing our full model (U → U), its specialist counterpart (U → S), and a purely specialized baseline (S → S), revealing two distinct patterns:

**Table 4. Superiority of the Unified Paradigm.** We disentangle the effects of unified training from unified inference by comparing our full model ( $\mathbf{U} \rightarrow \mathbf{U}$ ) against specialist configurations ( $\mathbf{U} \rightarrow \mathbf{S}$  and  $\mathbf{S} \rightarrow \mathbf{S}$ ).

Configuration	Overall Edit		Reading Order Edit		Detection (F1)
	EN	CH	EN	CH	
$\mathbf{U} \rightarrow \mathbf{U}$	<b>0.143</b>	<b>0.187</b>	<b>0.045</b>	<b>0.086</b>	0.820
$\mathbf{U} \rightarrow \mathbf{S}$	0.148	0.204	0.055	0.103	0.829
$\mathbf{S} \rightarrow \mathbf{S}$	<b>0.143</b>	0.211	0.058	0.108	<b>0.832</b>

**(1) Superiority in Context-Rich Tasks.** For text recognition and reading order, a clear hierarchy emerges:  $\mathbf{U} \rightarrow \mathbf{U} > \mathbf{U} \rightarrow \mathbf{S} > \mathbf{S} \rightarrow \mathbf{S}$ . The crucial comparison is between  $\mathbf{U} \rightarrow \mathbf{S}$  and  $\mathbf{S} \rightarrow \mathbf{S}$ . The jointly-trained  $\mathbf{U} \rightarrow \mathbf{S}$  model consistently outperforms the  $\mathbf{S} \rightarrow \mathbf{S}$  baseline (e.g., Overall Edit on Chinese drops from 0.211 to 0.204), providing direct evidence that unified training alone imbues the model with superior contextual awareness. The fully unified  $\mathbf{U} \rightarrow \mathbf{U}$  model further extends this lead, confirming that both joint training and joint inference contribute to peak performance.

**(2) Stability in Pure Localization.** In contrast, for the pure detection task, performance is remarkably stable across all three configurations. The specialized  $\mathbf{S} \rightarrow \mathbf{S}$  model achieves a marginally higher detection score (0.832 vs. 0.829 for  $\mathbf{U} \rightarrow \mathbf{S}$ ). This minimal difference suggests that while specialized training can narrowly optimize for localization, this task is not meaningfully compromised within our richer, joint-training framework.

In aggregate, these results show that while a specialized model holds a negligible edge in detection, our unified paradigm yields substantial gains in the more complex tasks of recognition and relational understanding. This superiority stems from the richer contextual representation forged through joint learning—a prerequisite for true document comprehension.

### 5.3. Effectiveness of the Holistic Data Engine

To validate the data engine’s effectiveness, we conduct a systematic ablation study. For this purpose, We focus on three critical types of data generated by our engine, each targeting a key challenge in document understanding:

- **D-Multilingual:** The full dataset excluding the Unified Multilingual Data. This variant is trained without synthetic documents spanning 100+ languages, allowing us to measure the impact on multilingual generalization.
- **D-Structured:** The full dataset excluding the Structured Data. This ablates the specialized set rich in complex tables and formulas, testing the model’s fine-grained parsing capabilities.
- **D-Correction:** Isolates the impact of the targeted correction data on overall performance

The results in Table 5 reveal a clear hierarchy of impact

**Table 5. Ablation study on our data engine.** We quantify the impact of each data pillar by removing it from the full training configuration.

Configuration	Overall Edit		Reading Order		Detection (F1)
	EN	CH	EN	CH	
<b>dots.ocr (Full)</b>	<b>0.125</b>	<b>0.160</b>	<b>0.040</b>	<b>0.067</b>	<b>0.849</b>
D-Multilingual	0.135	0.171	0.051	0.083	0.811
D-Structured	0.145	0.181	0.047	0.073	0.820
D-Correction	0.136	0.183	0.045	0.093	0.788

among our data pillars, while simultaneously underscoring that each is indispensable.

The most dramatic impact comes from ablating the targeted correction data (**w/o D-Correction**). This single change causes a catastrophic drop in detection performance, with the detection score plummeting from 0.849 to 0.788. This provides unequivocal evidence that our target correction loop is the critical mechanism for patching the model’s perceptual weaknesses and achieving high-fidelity localization.

While not as dramatic, the removal of the other two pillars reveals their distinct and vital roles. Ablating the structured data (**w/o D-Structured**) disproportionately harms the model’s ability to parse complex Chinese documents (Overall Edit degrades from 0.160 to 0.181), confirming this data’s crucial role in teaching structural understanding. Similarly, removing the multilingual data (**w/o D-Multilingual**) leads to a broad degradation across all metrics, highlighting its foundational importance for building a robust, cross-lingually capable model.

In summary, these ablations demonstrate that our model’s performance stems not from any single data source, but from the synergistic effect of our holistic data engine. Its components play distinct, complementary roles to forge a comprehensively robust model, ensuring high fidelity across a vast spectrum of languages, layouts, and complexities.

## 6. Conclusion

In this work, we presented dots.ocr, a unified model powered by a holistic data engine. Its architecture and data engine have enabled it to establish state-of-the-art performance across extensive benchmarks. Beyond its immediate performance, we argue that the true significance of this work lies in its potential to fuel the next generation of Vision-Language Models. By holistically parsing vast document corpora, dots.ocr can serve as a powerful data engine, unlocking novel pre-training tasks on rich, structured, and grounded data. We believe this is a pivotal step towards teaching VLMs to not merely see pixels, but to truly comprehend the world’s structured knowledge. As we posited in

the main paper’s conclusion, the ultimate value of dots.ocr extends beyond its state-of-the-art performance on document analysis benchmarks. We argued that its true significance lies in its potential to serve as a powerful data engine to fuel the next generation of Vision-Language Models (VLMs). In this section, we provide a detailed elaboration of this vision.

## References

- [1] Syeda Nahida Akter, Zichun Yu, Aashiq Muhamed, Tianyue Ou, Alex Bäuerle, Ángel Alexander Cabrera, Krish Dhakia, Chenyan Xiong, and Graham Neubig. An in-depth look at gemini’s language abilities. *arXiv preprint arXiv:2312.11444*, 2023. 3
- [2] Shuai Bai, Kebin Chen, Xuejing Liu, Jialin Wang, Wenbin Ge, Sibo Song, Kai Dang, Peng Wang, Shijie Wang, Jun Tang, et al. Qwen2. 5-vl technical report. *arXiv preprint arXiv:2502.13923*, 2025. 2, 3, 4, 5, 6, 12
- [3] Lukas Blecher, Guillem Cucurull, Thomas Scialom, and Robert Stojnic. Nougat: Neural optical understanding for academic documents. *arXiv preprint arXiv:2308.13418*, 2023. 2, 6
- [4] breezedeus. Pix2text: An open-source python3 tool for recognizing layouts, tables, math formulas (latex), and text in images. <https://github.com/breezedeus/pix2text>, 2025. 6
- [5] Hiuyi Cheng, Peirong Zhang, Sihang Wu, Jiaxin Zhang, Qiyuan Zhu, Zecheng Xie, Jing Li, Kai Ding, and Lianwen Jin. M6doc: A large-scale multi-format, multi-type, multi-layout, multi-language, multi-annotation category dataset for modern document layout analysis. In *Proceedings of the IEEE/CVF Conference on Computer Vision and Pattern Recognition*, pages 15138–15147, 2023. 3
- [6] Gheorghe Comanici, Eric Bieber, Mike Schaeckermann, Ice Pasupat, Noveen Sachdeva, Inderjit Dhillon, Marcel Blissein, Ori Ram, Dan Zhang, Evan Rosen, et al. Gemini 2.5: Pushing the frontier with advanced reasoning, multimodality, long context, and next generation agentic capabilities. *arXiv preprint arXiv:2507.06261*, 2025. 2, 5, 6, 12
- [7] Cheng Cui, Ting Sun, Manhui Lin, Tingquan Gao, Yubo Zhang, Jiaxuan Liu, Xueqing Wang, Zelun Zhang, Changda Zhou, Hongen Liu, et al. Paddleocr 3.0 technical report. *arXiv preprint arXiv:2507.05595*, 2025. 1, 6
- [8] Cheng Da, Chuwei Luo, Qi Zheng, and Cong Yao. Vision grid transformer for document layout analysis. In *Proceedings of the IEEE/CVF international conference on computer vision*, pages 19462–19472, 2023. 3
- [9] Mostafa Dehghani, Basil Mustafa, Josip Djolonga, Jonathan Heek, Matthias Minderer, Mathilde Caron, Andreas Steiner, Joan Puigcerver, Robert Geirhos, Ibrahim M Alabdulmohsin, et al. Patch n’pack: Navit, a vision transformer for any aspect ratio and resolution. *Advances in Neural Information Processing Systems*, 36:2252–2274, 2023. 3
- [10] Yongkun Du, Zhineng Chen, Hongtao Xie, Caiyan Jia, and Yu-Gang Jiang. Svtrv2: Ctc beats encoder-decoder models in scene text recognition. In *Proceedings of the IEEE/CVF International Conference on Computer Vision*, pages 20147–20156, 2025. 1
- [11] Hao Feng, Shu Wei, Xiang Fei, Wei Shi, Yingdong Han, Lei Liao, Jinghui Lu, Binghong Wu, Qi Liu, Chunhui Lin, et al. Dolphin: Document image parsing via heterogeneous anchor prompting. *arXiv preprint arXiv:2505.14059*, 2025. 3, 6
- [12] Sergey Filimonov. Open parse: Visually-driven document chunking for llm applications. <https://github.com/Filimoa/open-parse>, 2025. 6
- [13] Dong Guo, Faming Wu, Feida Zhu, Fuxing Leng, Guang Shi, Haobin Chen, Haoqi Fan, Jian Wang, Jianyu Jiang, Jiawei Wang, et al. Seed1. 5-vl technical report. *arXiv preprint arXiv:2505.07062*, 2025. 5, 6
- [14] Yupan Huang, Tengchao Lv, Lei Cui, Yutong Lu, and Furu Wei. Layoutlmv3: Pre-training for document ai with unified text and image masking. In *Proceedings of the 30th ACM international conference on multimedia*, pages 4083–4091, 2022. 1
- [15] Aaron Hurst, Adam Lerer, Adam P Goucher, Adam Perelman, Aditya Ramesh, Aidan Clark, AJ Ostrow, Akila Welihinda, Alan Hayes, Alec Radford, et al. Gpt-4o system card. *arXiv preprint arXiv:2410.21276*, 2024. 2, 6, 12
- [16] Geewook Kim, Teakgyu Hong, Moonbin Yim, Jinyoung Park, Jinyeong Yim, Wonseok Hwang, Sangdoo Yun, Dongyoon Han, and Seunghyun Park. Donut: Document understanding transformer without ocr. *arXiv preprint arXiv:2111.15664*, 7(15):2, 2021. 2
- [17] Zhanghui Kuang, Hongbin Sun, Zhizhong Li, Xiaoyu Yue, Tsui Hin Lin, Jianyong Chen, Huaqiang Wei, Yiqin Zhu, Tong Gao, Wenwei Zhang, et al. Mmocr: a comprehensive toolbox for text detection, recognition and understanding. In *Proceedings of the 29th ACM International Conference on Multimedia*, pages 3791–3794, 2021. 1
- [18] Hang Li. Cdla: A chinese document layout analysis (cdla) dataset, 2021. dataset. 3
- [19] Zhang Li, Yuliang Liu, Qiang Liu, Zhiyin Ma, Ziyang Zhang, Shuo Zhang, Zidun Guo, Jiarui Zhang, Xinyu Wang, and Xiang Bai. Monkeyocr: Document parsing with a structure-recognition-relation triplet paradigm. *arXiv preprint arXiv:2506.05218*, 2025. 3, 5, 6, 12
- [20] Nikolaos Livathinos, Christoph Auer, Maksym Lysak, Ahmed Nassar, Michele Dolfi, Panos Vagenas, Cesar Berrospi Ramis, Matteo Omenetti, Kasper Dinkla, Yusik Kim, et al. Docling: An efficient open-source toolkit for ai-driven document conversion. *arXiv preprint arXiv:2501.17887*, 2025. 6
- [21] Ilya Loshchilov and Frank Hutter. Decoupled weight decay regularization. *arXiv preprint arXiv:1711.05101*, 2017. 5
- [22] Souvik Mandal, Ashish Talewar, Paras Ahuja, and Prathamesh Juvatkar. Nanonets-ocr-s: A model for transforming documents into structured markdown with intelligent content recognition and semantic tagging, 2025. 12
- [23] Simone Marinai and Hiromichi Fujisawa. *Machine learning in document analysis and recognition*. Springer, 2007. 1
- [24] Minesh Mathew, Dimosthenis Karatzas, and CV Jawahar. Docvqa: A dataset for vqa on document images. In *Proceedings of the IEEE/CVF winter conference on applications of computer vision*, pages 2200–2209, 2021. 1

- [25] Mathpix. Mathpix: Ocr and document conversion for scientific pdfs. <https://mathpix.com/>, 2024. Accessed: 2024-06-10. 6
- [26] Ahmed Nassar, Andres Marafioti, Matteo Omenetti, Maksym Lysak, Nikolaos Livathinos, Christoph Auer, Lucas Morin, Rafael Teixeira de Lima, Yusik Kim, A Said Gurbuz, et al. Smoldocling: An ultra-compact vision-language model for end-to-end multi-modal document conversion. *arXiv preprint arXiv:2503.11576*, 2025. 6
- [27] OCRFlux. Ocrflux. <https://github.com/chatdoc-com/OCRFlux>, 2025. 6
- [28] Elsa A Olivetti, Jacqueline M Cole, Edward Kim, Olga Kononova, Gerbrand Ceder, Thomas Yong-Jin Han, and Anna M Hiszpanski. Data-driven materials research enabled by natural language processing and information extraction. *Applied Physics Reviews*, 7(4), 2020. 1
- [29] Linke Ouyang, Yuan Qu, Hongbin Zhou, Jiawei Zhu, Rui Zhang, Qunshu Lin, Bin Wang, Zhiyuan Zhao, Man Jiang, Xiaomeng Zhao, et al. Omnidocbench: Benchmarking diverse pdf document parsing with comprehensive annotations. In *Proceedings of the Computer Vision and Pattern Recognition Conference*, pages 24838–24848, 2025. 1, 2, 3, 5, 7
- [30] Shubham Singh Paliwal, D Vishwanath, Rohit Rahul, Monika Sharma, and Lovekesh Vig. Tablenet: Deep learning model for end-to-end table detection and tabular data extraction from scanned document images. In *2019 international conference on document analysis and recognition (ICDAR)*, pages 128–133. IEEE, 2019. 1
- [31] Vik Paruchuri. Marker, 2024. 6, 12
- [32] Dezhi Peng, Xinyu Wang, Yuliang Liu, Jiaxin Zhang, Mingxin Huang, Songxuan Lai, Jing Li, Shenggao Zhu, Dahua Lin, Chunhua Shen, et al. Spts: single-point text spotting. In *Proceedings of the 30th ACM International Conference on Multimedia*, pages 4272–4281, 2022. 2
- [33] Birgit Pfitzmann, Christoph Auer, Michele Dolfi, Ahmed S Nassar, and Peter Staar. Doclaynet: A large human-annotated dataset for document-layout segmentation. In *Proceedings of the 28th ACM SIGKDD conference on knowledge discovery and data mining*, pages 3743–3751, 2022. 3
- [34] Jake Poznanski, Aman Rangapur, Jon Borchardt, Jason Dunkelberger, Regan Huff, Daniel Lin, Christopher Wilhelm, Kyle Lo, and Luca Soldaini. olmocr: Unlocking trillions of tokens in pdfs with vision language models. *arXiv preprint arXiv:2502.18443*, 2025. 1, 3, 5, 6, 12
- [35] Chenfan Qu, Chongyu Liu, Yuliang Liu, Xinhong Chen, Dezhi Peng, Fengjun Guo, and Lianwen Jin. Towards robust tampered text detection in document image: New dataset and new solution. In *Proceedings of the IEEE/CVF Conference on Computer Vision and Pattern Recognition*, pages 5937–5946, 2023. 1
- [36] Oleksii Sidorov, Ronghang Hu, Marcus Rohrbach, and Amanpreet Singh. Textcaps: a dataset for image captioning with reading comprehension. In *European conference on computer vision*, pages 742–758. Springer, 2020. 1
- [37] Amanpreet Singh, Vivek Natarajan, Meet Shah, Yu Jiang, Xinlei Chen, Dhruv Batra, Devi Parikh, and Marcus Rohrbach. Towards vqa models that can read. In *Proceedings of the IEEE/CVF conference on computer vision and pattern recognition*, pages 8317–8326, 2019. 1
- [38] Ray Smith. An overview of the tesseract ocr engine. In *Ninth international conference on document analysis and recognition (ICDAR 2007)*, pages 629–633. IEEE, 2007. 1
- [39] Mistral AI Team. Mistral-ocr. <https://mistral.ai/news/mistral-ocr>, 2025. Accessed via ai-bot.cn. 6, 12
- [40] Unstructured-IO. unstructured. <https://github.com/Unstructured-IO/unstructured>, 2024. Accessed: 2024-06-10. 6
- [41] Jianqiang Wan, Sibo Song, Wenwen Yu, Yuliang Liu, Wenzheng Cheng, Fei Huang, Xiang Bai, Cong Yao, and Zhibo Yang. Omniparser: A unified framework for text spotting key information extraction and table recognition. In *Proceedings of the IEEE/CVF conference on computer vision and pattern recognition*, pages 15641–15653, 2024. 2
- [42] Bin Wang, Chao Xu, Xiaomeng Zhao, Linke Ouyang, Fan Wu, Zhiyuan Zhao, Rui Xu, Kaiwen Liu, Yuan Qu, Fukai Shang, et al. Mineru: An open-source solution for precise document content extraction. *arXiv preprint arXiv:2409.18839*, 2024. 1, 6, 12
- [43] Dongsheng Wang, Natraj Raman, Mathieu Sibue, Zhiqiang Ma, Petr Babkin, Simerjot Kaur, Yulong Pei, Armineh Nourbakhsh, and Xiaomo Liu. Docilm: A layout-aware generative language model for multimodal document understanding. In *Proceedings of the 62nd annual meeting of the association for computational linguistics (volume 1: long papers)*, pages 8529–8548, 2024. 2
- [44] Peng Wang, Shuai Bai, Sinan Tan, Shijie Wang, Zhihao Fan, Jinze Bai, Keqin Chen, Xuejing Liu, Jialin Wang, Wenbin Ge, et al. Qwen2-vl: Enhancing vision-language model's perception of the world at any resolution. *arXiv preprint arXiv:2409.12191*, 2024. 1, 6, 12
- [45] Zilong Wang, Yiheng Xu, Lei Cui, Jingbo Shang, and Furu Wei. Layoutreader: Pre-training of text and layout for reading order detection. *arXiv preprint arXiv:2108.11591*, 2021. 1
- [46] Haoran Wei, Chenglong Liu, Jinyue Chen, Jia Wang, Lingyu Kong, Yanming Xu, Zheng Ge, Liang Zhao, Jianjian Sun, Yuang Peng, et al. General ocr theory: Towards ocr-2.0 via a unified end-to-end model. *arXiv preprint arXiv:2409.01704*, 2024. 6, 12
- [47] Renqiu Xia, Song Mao, Xiangchao Yan, Hongbin Zhou, Bo Zhang, Haoyang Peng, Jiahao Pi, Daocheng Fu, Wennejie Wu, Hancheng Ye, et al. Docgenome: An open large-scale scientific document benchmark for training and testing multi-modal large language models. *arXiv preprint arXiv:2406.11633*, 2024. 3
- [48] Yiheng Xu, Minghao Li, Lei Cui, Shaohan Huang, Furu Wei, and Ming Zhou. Layoutlm: Pre-training of text and layout for document image understanding. In *Proceedings of the 26th ACM SIGKDD international conference on knowledge discovery & data mining*, pages 1192–1200, 2020. 1
- [49] Yiheng Xu, Tengchao Lv, Lei Cui, Guoxin Wang, Yijuan Lu, Dinei Florencio, Cha Zhang, and Furu Wei. Xfund: A benchmark dataset for multilingual visually rich form understanding. In *Findings of the association for computational linguistics: ACL 2022*, pages 3214–3224, 2022. 1

- [50] Chong Zhang, Ya Guo, Yi Tu, Huan Chen, Jinyang Tang, Huijia Zhu, Qi Zhang, and Tao Gui. Reading order matters: Information extraction from visually-rich documents by token path prediction. *arXiv preprint arXiv:2310.11016*, 2023.  
[1](#)
- [51] Yian Zhao, Wenyu Lv, Shangliang Xu, Jinman Wei, Guanzhong Wang, Qingqing Dang, Yi Liu, and Jie Chen. Detrs beat yolos on real-time object detection. In *Proceedings of the IEEE/CVF conference on computer vision and pattern recognition*, pages 16965–16974, 2024. [1](#)
- [52] Xu Zhong, Jianbin Tang, and Antonio Jimeno Yepes. Publaynet: largest dataset ever for document layout analysis. In *2019 International conference on document analysis and recognition (ICDAR)*, pages 1015–1022. IEEE, 2019. [1](#)

# dots.ocr: Multilingual Document Layout Parsing in a Single Vision-Language Model

## Supplementary Material

### 7. Supporting Results on olmOCR-Bench

In this section, we further verify the performance of our model by presenting supplementary end-to-end evaluation results on the olmOCR-Bench benchmark [34], complementing the main findings reported in the paper. Detailed results of dots.ocr and various baselines are shown in Table 6.

Table 6. Detailed comparison on the **olmOCR-Bench** [34] benchmark. All scores are reported as a percentage (%), where higher is better.

Model	ArXiv	Old Scans	Math	Tables	Old Scans	Headers and Footers	Multi column	Long Text	Tiny Text	Base	Overall
GOT-OCR [46]	52.7	52.0	0.2	22.1	93.6	42.0	29.9	94.0	48.3 ± 1.1		
Marker [31]	76.0	57.9	57.6	27.8	84.9	72.9	84.6	99.1	70.1 ± 1.1		
MinerU [42]	75.4	47.4	60.9	17.3	<b>96.6</b>	59.0	39.1	96.6	61.5 ± 1.1		
Mistral OCR [39]	77.2	67.5	60.6	29.3	93.6	71.3	77.1	99.4	72.0 ± 1.1		
Nanonet OCR [22]	67.0	68.6	77.7	39.5	40.7	69.9	53.4	99.3	64.5 ± 1.1		
GPT4o (No Anchor) [15]	51.5	<b>75.5</b>	69.1	40.9	94.2	68.9	54.1	96.7	68.9 ± 1.1		
GPT4o (Anchored) [15]	53.5	74.5	70.0	40.7	93.8	69.3	60.6	96.8	69.9 ± 1.1		
Gemini Flash 2 (No Anchor) [6]	32.1	56.3	61.4	27.8	48.0	58.7	<b>84.4</b>	94.0	57.8 ± 1.1		
Gemini Flash 2 (Anchored) [6]	54.5	56.1	72.1	34.2	64.7	61.5	71.5	95.6	63.8 ± 1.2		
Qwen2-VL-72B (No Anchor) [44]	19.7	31.7	24.2	17.1	88.9	8.3	6.8	55.5	31.5 ± 0.9		
Qwen2.5-VL-72B (No Anchor) [2]	63.1	65.7	67.3	38.6	73.6	68.3	49.1	98.3	65.5 ± 1.2		
olmOCR v0.1.75 (No Anchor) [34]	71.5	71.4	71.4	<b>42.8</b>	94.1	77.7	71.0	97.8	74.7 ± 1.1		
olmOCR v0.1.75 (Anchored) [34]	74.9	71.2	71.0	42.2	94.5	78.3	73.3	98.3	75.5 ± 1.0		
MonkeyOCR-pro-3B [19]	<b>83.8</b>	68.8	74.6	36.1	91.2	76.6	80.1	95.3	75.8 ± 1.0		
<b>dots.ocr (Ours)</b>	82.1	64.2	<b>88.3</b>	40.9	94.1	<b>82.4</b>	81.2	<b>99.5</b>	<b>79.1 ± 1.0</b>		

### 8. Layout Detection Metric

In this section, We introduce a confidence-free, F1-score-based evaluation metric that is more robust and provides a fairer assessment of layout detection performance.

**Core Idea.** The core idea is a two-stage matching process. The first stage handles clear one-to-one matches between predicted and ground-truth boxes. The second stage addresses more complex scenarios, such as one-to-many or many-to-many relationships, by first clustering spatially related boxes into larger “super-boxes” and then attempting to match them. This approach allows the metric to correctly reward a model that, for example, predicts three separate lines for a paragraph that is annotated as a single block in the ground truth.

**Category-Aware and Category-Agnostic Modes.** Our evaluation metric supports two modes. In the *category-aware* mode, all operations (matching and clustering) are carried out within each annotation category, only boxes of the same category are matched together. The True Positives (TPs), False Positives (FPs), and False Negatives (FNs) are counted for each category, and then aggregated. In the *category-agnostic* mode, the process ignores box categories, treating all boxes as a single group. This flexibility allows evaluation of either pure layout prediction quality or joint layout and category performance.

**Two-Stage Matching Process.** The evaluation logic is detailed in Algorithm 1. It proceeds as follows:

**Stage 1: One-to-One Matching.** We first perform an optimal bipartite matching between the set of all predicted boxes ( $\mathcal{P}$ ) and all ground-truth boxes ( $\mathcal{G}$ ) using the Hungarian algorithm on an IoU-based cost matrix. Matched pairs with an IoU greater than a predefined threshold (e.g., 0.5) are counted as initial TPs. These matched boxes are then removed from their respective sets, leaving unmatched predicted boxes ( $\mathcal{P}'$ ) and unmatched ground-truth boxes ( $\mathcal{G}'$ ).

**Stage 2: Matching via Clustering.** The remaining unmatched boxes,  $\mathcal{P}'$  and  $\mathcal{G}'$ , are processed independently. We apply a clustering algorithm to each set. This algorithm groups spatially adjacent boxes based on geometric heuristics (e.g., high vertical overlap and small horizontal gap for line merging, followed by high horizontal overlap and small vertical gap for

paragraph merging). This step results in a set of merged predicted boxes ( $\mathcal{P}_{merged}$ ) and merged ground-truth boxes ( $\mathcal{G}_{merged}$ ). We then perform a second round of optimal bipartite matching on these merged sets. Pairs with an IoU above the threshold contribute additional TPs.

**Final Calculation.** After the second stage, any remaining unmatched boxes in  $\mathcal{P}_{merged}$  are counted as FPs, and any remaining boxes in  $\mathcal{G}_{merged}$  are counted as FNs. The total TPs, FPs, and FNs are then used to calculate the final Precision, Recall, and F1-score.

---

**Algorithm 1:** Layout Detection Metric

---

**Input:** Predicted boxes  $\mathcal{P}$ , Ground-truth boxes  $\mathcal{G}$ , IoU threshold  $\tau$

**Output:** Precision, Recall, F1-score

```

// Stage 1: One-to-one matching
1  $M_1 \leftarrow \text{OptimalBipartiteMatch}(\mathcal{P}, \mathcal{G})$                                 // Using Hungarian algorithm on IoU
2  $TP_1 \leftarrow 0$ 
3  $\mathcal{P}_{matched} \leftarrow \emptyset, \mathcal{G}_{matched} \leftarrow \emptyset$ 
4 foreach match  $(p, g) \in M_1$  do
5   if  $IoU(p, g) \geq \tau$  then
6      $TP_1 \leftarrow TP_1 + 1$ 
7      $\mathcal{P}_{matched} \leftarrow \mathcal{P}_{matched} \cup \{p\}$ 
8      $\mathcal{G}_{matched} \leftarrow \mathcal{G}_{matched} \cup \{g\}$ 
9   end
10 end
11  $\mathcal{P}' \leftarrow \mathcal{P} \setminus \mathcal{P}_{matched}$                                          // Unmatched predicted boxes
12  $\mathcal{G}' \leftarrow \mathcal{G} \setminus \mathcal{G}_{matched}$                                          // Unmatched ground-truth boxes

// Stage 2: Matching after clustering
13  $\mathcal{P}_{merged} \leftarrow \text{ClusterBoxes}(\mathcal{P}')$                                      // Merge adjacent boxes in  $\mathcal{P}'$ 
14  $\mathcal{G}_{merged} \leftarrow \text{ClusterBoxes}(\mathcal{G}')$                                      // Merge adjacent boxes in  $\mathcal{G}'$ 

15  $M_2 \leftarrow \text{OptimalBipartiteMatch}(\mathcal{P}_{merged}, \mathcal{G}_{merged})$ 
16  $TP_2 \leftarrow 0$ 
17  $\mathcal{P}_{merged\_matched} \leftarrow \emptyset, \mathcal{G}_{merged\_matched} \leftarrow \emptyset$ 
18 foreach match  $(p_m, g_m) \in M_2$  do
19   if  $IoU(p_m, g_m) \geq \tau$  then
20      $TP_2 \leftarrow TP_2 + 1$ 
21      $\mathcal{P}_{merged\_matched} \leftarrow \mathcal{P}_{merged\_matched} \cup \{p_m\}$ 
22      $\mathcal{G}_{merged\_matched} \leftarrow \mathcal{G}_{merged\_matched} \cup \{g_m\}$ 
23   end
24 end

// Final Calculation
25  $TP_{total} \leftarrow TP_1 + TP_2$ 
26  $FP \leftarrow |\mathcal{P}_{merged}| - |\mathcal{P}_{merged\_matched}|$ 
27  $FN \leftarrow |\mathcal{G}_{merged}| - |\mathcal{G}_{merged\_matched}|$ 
28  $Precision \leftarrow TP_{total}/(TP_{total} + FP)$ 
29  $Recall \leftarrow TP_{total}/(TP_{total} + FN)$ 
30  $F1 \leftarrow 2 \times (Precision \times Recall)/(Precision + Recall)$ 
31 return  $Precision, Recall, F1$ 

```

---

## 9. Qualitative Analysis of Ablation Studies

In this section, we provide qualitative examples that visually complement the quantitative results presented in our ablation study. These examples are chosen to vividly illustrate the core findings of our investigation, particularly the nuanced roles of

text recognition and reading order within our unified framework.

As argued in the main text, while ablating text recognition ( $M_{\text{Rec}}$ ) may lead to a marginal improvement in the isolated detection metric, it comes at the cost of semantic understanding and end-to-end performance. Qualitative comparisons in Figures 3–6 visually highlight this degradation. Specifically, the absence of recognition supervision results in detections misaligned with the logical structure of the text, causing fragmented bounding boxes and incorrect reading orders.

We further present two qualitative examples obtained by ablating the reading order supervision ( $M_{\text{RO}}$ ). As shown in Figure 7, the absence of this guidance results in misaligned bounding regions. Furthermore, Figure 8 reveals a critical failure where the model cannot discern four independent tables, erroneously aggregating them into a single, spanning box.

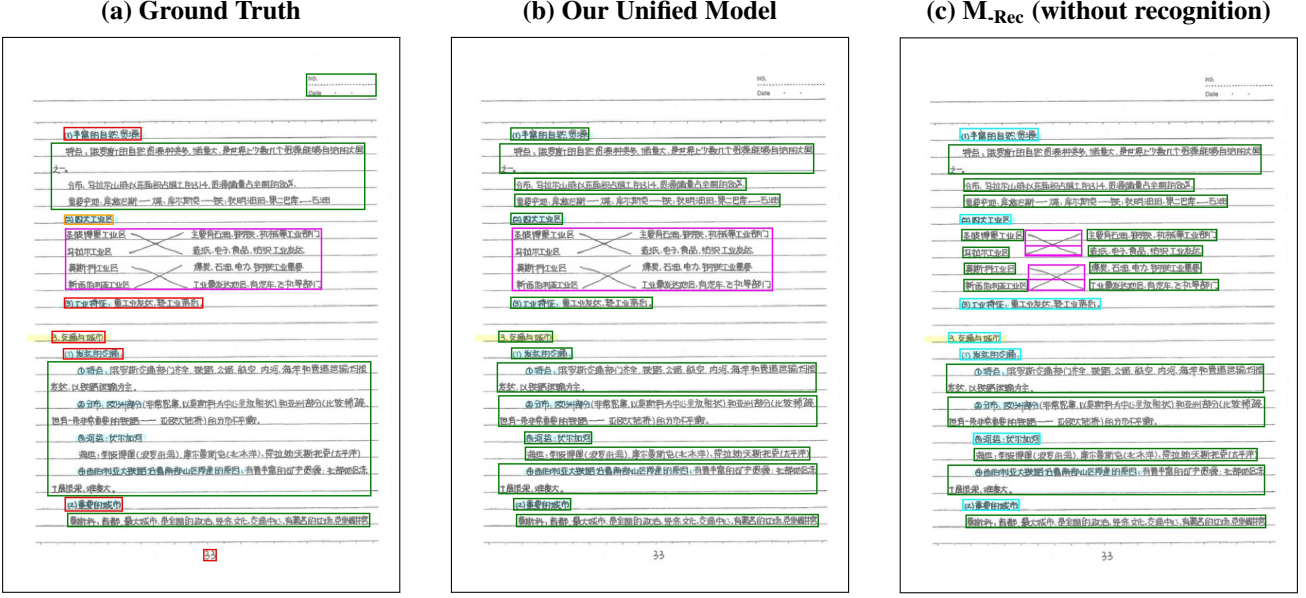


Figure 3. **Effect of Removing the Recognition task (1).** (a) Ground Truth. (b) Output of our model under the unified training paradigm, which correctly preserves the entire connected diagram as a single coherent structure. (c) Output of the model without the recognition task. Unlike (b), the ablated model breaks the originally unified connected diagram into many isolated fragments, treating each short stroke or text segment as an individual object. This demonstrates that the recognition task provides essential semantic constraints that prevent such structural fragmentation.

## 10. dots.ocr as a Data Engine for VLM training

As we posited in the main paper, the ultimate value of dots.ocr extends beyond its excellent performance on document analysis benchmarks. Its true significance lies in serving as a powerful data engine to fuel the next generation of VLMs. Here, we elaborate on this premise and substantiate its broader implications.

We recognize that documents serve as a vast, untapped reservoir of human knowledge. dots.ocr acts as a pivotal tool to unlock this wealth, enabling the efficient extraction of high-quality multimodal information for VLM training. Specifically, our system facilitates a diverse array of downstream tasks: for lengthy volumes such as books with thousands of pages, it extracts coherent long-context textual narratives; it provides precise bounding box annotations to enhance the model’s visual grounding capabilities; it mines rich image-caption pairs interleaved within the text; and it supports advanced generative objectives, including visual text inpainting and next-page text prediction. Figures 9–13 visually exemplify these capabilities, showcasing the quality and diversity of the training data generated by our model.

### (a) Ground Truth

MONEY		GEMS	
EQUIPMENT			
1			
2			
3			
4			
5			
6			
7	+1 Enc.		
8			
9			
10			
11	+1 Enc.		
12			
13			
14			
15			
16	+1 Enc.		
17			
18			
19			
20			
21	+1 Enc.		
22			
23			
24			
25			
26			
27			
28			
29			
30			
31			
NON-ENCUMBERING EQUIPMENT			
PROPERTIES			
Name	Location	Value	
LIBRARY VALUE		LABORATORY VALUE	
INVESTMENTS			
Name	Type	Value	

### (b) Our Unified Model

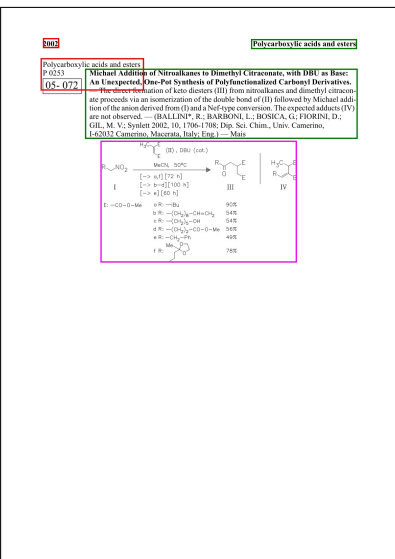
MONEY	GEMS	LANGUAGES	
EQUIPMENT		KNOWN	NOT KNOWN
1			
2			
3			
4			
5			
6	+1 Rue		
7	+1 Rue		
8	+1 Rue		
9	+1 Rue		
10	+1 Rue		
11	+1 Rue		
12	+1 Rue		
13	+1 Rue		
14	+1 Rue		
15	+1 Rue		
16	+1 Rue		
17	+1 Rue		
18	+1 Rue		
19	+1 Rue		
20	+1 Rue		
21	+1 Rue		
22	+1 Rue		
23	+1 Rue		
24	+1 Rue		
25	+1 Rue		
26		PROPERTIES	
27		Location	Value
28			
29			
30			
31			
		INVESTMENTS	
		Type	Value

**(c) M<sub>Rec</sub> (without recognition)**

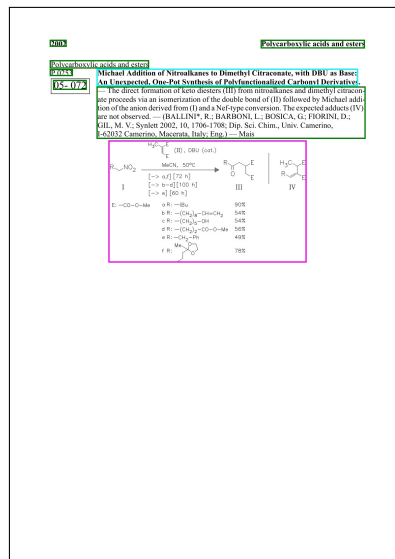
MONEY		ITEMS		LANGUAGES		NOT KNOWN	
EQUIPMENT							
1							
2							
3							
4							
5							
6		+1 Rune					
7							
8							
9							
10							
11							
12							
13							
14							
15							
16							
17							
18							
19							
20							
21		+1 Rune					
22							
23							
24							
25							
26							
27							
28							
29							
30							
31							

**Figure 4. Effect of Removing the Recognition task (2).** For the table in the lower-right region, (b) Our unified model correctly recognizes the entire table as a single structured layout, preserving its rows, columns, and bounding geometry. (c) In contrast, the model without the recognition objective fails to detect the table as a unified structure. Instead of capturing the table boundaries and grid lines, it isolates and boxes only the individual text tokens inside the table.

### (a) Ground Truth



### (b) Our Unified Model



### (c) M-Rec (without recognition)

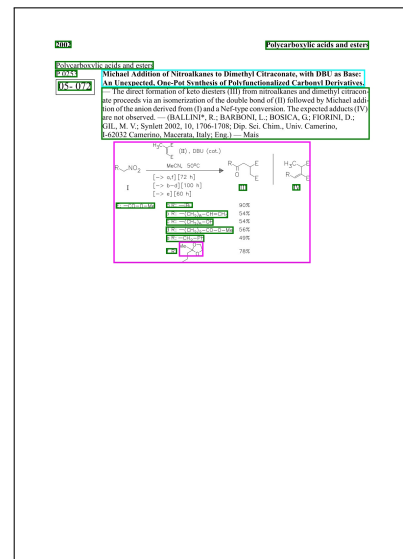


**Figure 5. Effect of Removing the Recognition task (3).** For the chemical reaction scheme in the lower region, (b) Our unified model detects the entire reaction diagram as a single, coherent figure, preserving its hierarchical structure where internal elements (chemical formulas, labels, yields, arrows) are treated as components of one unified visual unit. (c) Although the recognition-ablated model successfully delineates the overall diagram, it disrupts the internal hierarchy through excessive segmentation. By individually isolating text tokens, chemical formulas, and captions, the model produces a cluttered and structurally inconsistent interpretation.

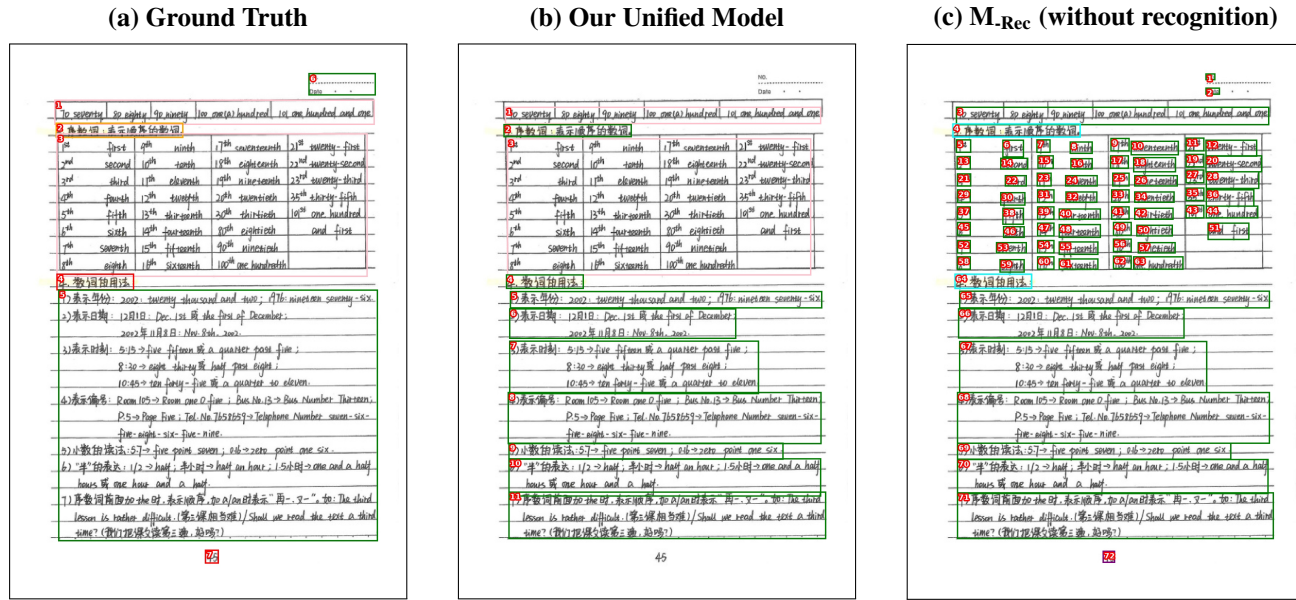


Figure 6. Effect of Removing the Recognition task (4). In the upper-left corner, the red numbers indicate the intended reading order of the paragraphs. (b) Our unified model detects the entire word table as a coherent structure, preserving its layout and correctly following the reading sequence. (c) Without recognition supervision, the model breaks the table into individual word elements, drawing separate boxes for each token. Moreover, it outputs these elements in a horizontal row-by-row sequence rather than the intended vertical order. This highlights the critical role of recognition in capturing high-level structural semantics.

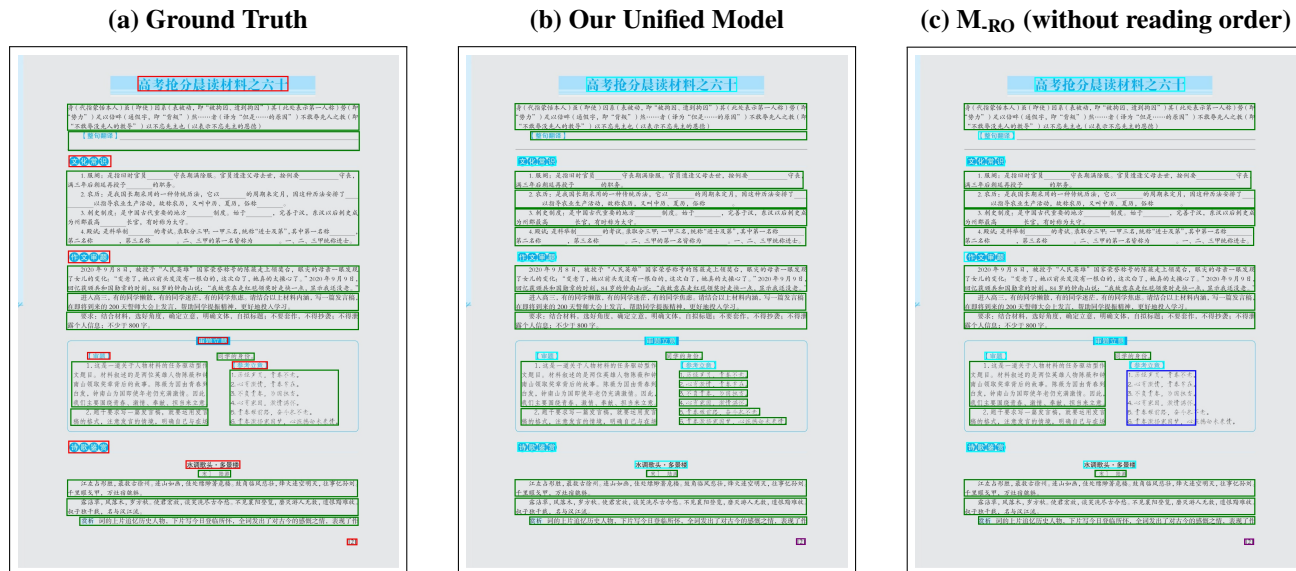
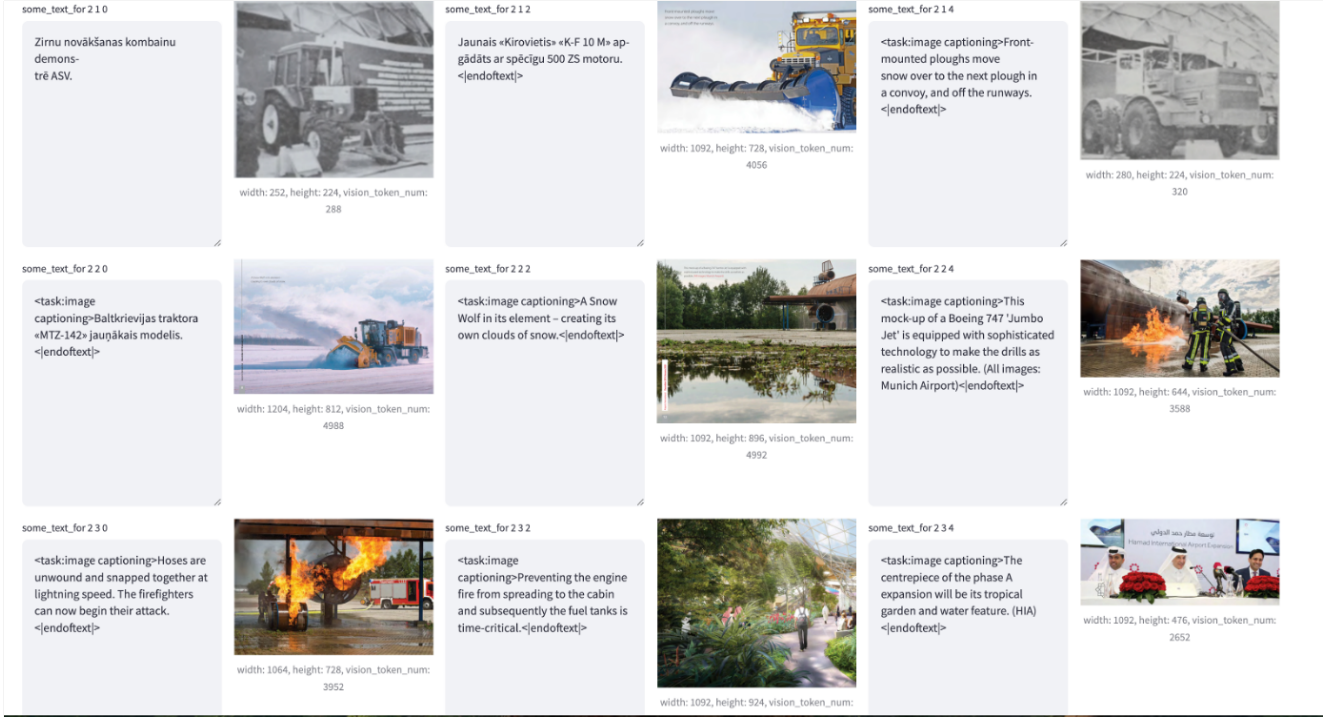


Figure 7. Effect of Removing reading order (1). (b) our unified model generates structurally coherent detection boxes that accurately encapsulate text groups. (c) Upon removing reading-order supervision, the generated detection boxes become misaligned. This underscores that proper reading-order supervision is vital for achieving accurate detection within a unified framework.

(a) Ground Truth

客户信息表									
客户基本信息					客户详细信息				
客户ID		客户姓名			客户性别		客户年龄		
客户ID	客户姓名	客户性别	客户年龄	客户地址	客户ID	客户姓名	客户年龄	客户地址	客户ID
10001	张三	男	35	北京市朝阳区	10002	李四	女	28	上海市浦东新区
10003	王五	男	42	广州市天河区	10004	赵六	女	30	深圳市南山区
10005	孙七	男	25	天津市和平区	10006	钱八	女	38	重庆市渝中区
10007	周九	男	32	武汉市江汉区	10008	吴十	女	29	长沙市雨花区
10009	郑十一	男	37	南京市鼓楼区	10010	胡十二	女	33	苏州市工业园区
10011	范十三	男	39	杭州市西湖区	10012	朱十四	女	31	宁波市鄞州区
10013	高十五	男	41	济南市历下区	10014	徐十六	女	35	青岛市市北区
10015	黄十七	男	43	郑州市中原区	10016	何十八	女	37	洛阳市涧西区
10017	黎十九	男	45	西安市碑林区	10018	段二十	女	39	西安市莲湖区
10019	侯二十一	男	47	西安市雁塔区	10020	魏二十二	女	41	西安市高新区
10021	侯二十三	男	49	西安市未央区	10022	侯二十四	女	43	西安市新城区
10023	侯二十五	男	51	西安市灞桥区	10024	侯二十六	女	45	西安市莲湖区
10025	侯二十七	男	53	西安市碑林区	10026	侯二十八	女	47	西安市雁塔区
10027	侯二十九	男	55	西安市未央区	10028	侯三十	女	49	西安市新城区
10029	侯三十一	男	57	西安市灞桥区	10030	侯三十二	女	51	西安市莲湖区
10031	侯三十三	男	59	西安市碑林区	10032	侯三十四	女	53	西安市雁塔区
10033	侯三十五	男	61	西安市未央区	10034	侯三十六	女	55	西安市新城区
10035	侯三十七	男	63	西安市灞桥区	10036	侯三十八	女	57	西安市莲湖区
10037	侯三十九	男	65	西安市碑林区	10038	侯四十	女	59	西安市雁塔区
10039	侯四十一	男	67	西安市未央区	10040	侯四十二	女	61	西安市新城区
10041	侯四十三	男	69	西安市灞桥区	10042	侯四十四	女	63	西安市莲湖区
10043	侯四十五	男	71	西安市碑林区	10044	侯四十六	女	65	西安市雁塔区
10045	侯四十七	男	73	西安市未央区	10046	侯四十八	女	67	西安市新城区
10047	侯四十九	男	75	西安市灞桥区	10048	侯五十	女	69	西安市莲湖区
10049	侯五十一	男	77	西安市碑林区	10050	侯五十二	女	71	西安市雁塔区
10051	侯五十三	男	79	西安市未央区	10052	侯五十四	女	73	西安市新城区
10053	侯五十五	男	81	西安市灞桥区	10054	侯五十六	女	75	西安市莲湖区
10055	侯五十七	男	83	西安市碑林区	10056	侯五十八	女	77	西安市雁塔区
10057	侯五十九	男	85	西安市未央区	10058	侯六十	女	79	西安市新城区
10059	侯六十一	男	87	西安市灞桥区	10060	侯六十二	女	81	西安市莲湖区
10061	侯六十三	男	89	西安市碑林区	10062	侯六十四	女	83	西安市雁塔区
10063	侯六十五	男	91	西安市未央区	10064	侯六十六	女	85	西安市新城区
10065	侯六十七	男	93	西安市灞桥区	10066	侯六十八	女	87	西安市莲湖区
10067	侯六十九	男	95	西安市碑林区	10068	侯七十	女	89	西安市雁塔区
10069	侯七十一	男	97	西安市未央区	10070	侯七十二	女	91	西安市新城区
10071	侯七十三	男	99	西安市灞桥区	10072	侯七十四	女	93	西安市莲湖区
10073	侯七十五	男	101	西安市碑林区	10074	侯七十六	女	95	西安市雁塔区
10075	侯七十七	男	103	西安市未央区	10076	侯七十八	女	97	西安市新城区
10077	侯七十九	男	105	西安市灞桥区	10078	侯八十	女	99	西安市莲湖区
10079	侯八十一	男	107	西安市碑林区	10080	侯八十二	女	101	西安市雁塔区
10081	侯八十三	男	109	西安市未央区	10082	侯八十四	女	103	西安市新城区
10083	侯八十五	男	111	西安市灞桥区	10084	侯八十六	女	105	西安市莲湖区
10085	侯八十七	男	113	西安市碑林区	10086	侯八十八	女	107	西安市雁塔区
10087	侯八十九	男	115	西安市未央区	10088	侯九十	女	109	西安市新城区
10089	侯九十一	男	117	西安市灞桥区	10090	侯九十二	女	111	西安市莲湖区
10091	侯九十三	男	119	西安市碑林区	10092	侯九十四	女	113	西安市雁塔区
10093	侯九十五	男	121	西安市未央区	10094	侯九十六	女	115	西安市新城区
10095	侯九十七	男	123	西安市灞桥区	10096	侯九十八	女	117	西安市莲湖区
10097	侯九十九	男	125	西安市碑林区	10098	侯一百	女	119	西安市雁塔区
10099	侯一百零一	男	127	西安市未央区	10100	侯一百零二	女	121	西安市新城区
10101	侯一百零三	男	129	西安市灞桥区	10102	侯一百零四	女	123	西安市莲湖区
10103	侯一百零五	男	131	西安市碑林区	10104	侯一百零六	女	125	西安市雁塔区
10105	侯一百零七	男	133	西安市未央区	10106	侯一百零八	女	127	西安市新城区
10107	侯一百零九	男	135	西安市灞桥区	10108	侯一百一十	女	129	西安市莲湖区
10109	侯一百一十一	男	137	西安市碑林区	10110	侯一百一十二	女	131	西安市雁塔区
10111	侯一百一十三	男	139	西安市未央区	10112	侯一百一十四	女	133	西安市新城区
10113	侯一百一十五	男	141	西安市灞桥区	10114	侯一百一十六	女	135	西安市莲湖区
10115	侯一百一十七	男	143	西安市碑林区	10116	侯一百一十八	女	137	西安市雁塔区
10117	侯一百一十九	男	145	西安市未央区	10118	侯一百二十	女	139	西安市新城区
10119	侯一百二十一	男	147	西安市灞桥区	10120	侯一百二十二	女	141	西安市莲湖区
10121	侯一百二十三	男	149	西安市碑林区	10122	侯一百二十四	女	143	西安市雁塔区
10123	侯一百二十五	男	151	西安市未央区	10124	侯一百二十六	女	145	西安市新城区
10125	侯一百二十七	男	153	西安市灞桥区	10126	侯一百二十八	女	147	西安市莲湖区
10127	侯一百二十九	男	155	西安市碑林区	10128	侯一百三十	女	149	西安市雁塔区
10129	侯一百三十一	男	157	西安市未央区	10130	侯一百三十二	女	151	西安市新城区
10131	侯一百三十三	男	159	西安市灞桥区	10132	侯一百三十四	女	153	西安市莲湖区
10133	侯一百三十五	男	161	西安市碑林区	10134	侯一百三十六	女	155	西安市雁塔区
10135	侯一百三十七	男	163	西安市未央区	10136	侯一百三十八	女	157	西安市新城区
10137	侯一百三十九	男	165	西安市灞桥区	10138	侯一百四十	女	159	西安市莲湖区
10139	侯一百四十一	男	167	西安市碑林区	10140	侯一百四十二	女	161	西安市雁塔区
10141	侯一百四十三	男	169	西安市未央区	10142	侯一百四十四	女	163	西安市新城区
10143	侯一百四十五	男	171	西安市灞桥区	10144	侯一百四十六	女	165	西安市莲湖区
10145	侯一百四十七	男	173	西安市碑林区	10146	侯一百四十八	女	167	西安市雁塔区
10147	侯一百四十九	男	175	西安市未央区	10148	侯一百五十	女	169	西安市新城区
10149	侯一百五十一	男	177	西安市灞桥区	10150	侯一百五十二	女	171	西安市莲湖区
10151	侯一百五十三	男	179	西安市碑林区	10152	侯一百五十四	女	173	西安市雁塔区
10153	侯一百五十五	男	181	西安市未央区	10154	侯一百五十六	女	175	西安市新城区
10155	侯一百五十七	男	183	西安市灞桥区	10156	侯一百五十八	女	177	西安市莲湖区
10157	侯一百五十九	男	185	西安市碑林区	10158	侯一百六十	女	179	西安市雁塔区
10159	侯一百六十一	男	187	西安市未央区	10160	侯一百六十二	女	181	西安市新城区
10161	侯一百六十三	男	189	西安市灞桥区	10162	侯一百六十四	女	183	西安市莲湖区
10163	侯一百六十五	男	191	西安市碑林区	10164	侯一百六十六	女	185	西安市雁塔区
10165	侯一百六十七	男	193	西安市未央区	10166	侯一百六十八	女	187	西安市新城区
10167	侯一百六十九	男	195	西安市灞桥区	10168	侯一百七十	女	189	西安市莲湖区
10169	侯一百七十一	男	197	西安市碑林区	10170	侯一百七十二	女	191	西安市雁塔区
10171	侯一百七十三	男	199	西安市未央区	10172	侯一百七十四	女	193	西安市新城区
10173	侯一百七十五	男	201	西安市灞桥区	10174	侯一百七十六	女	195	西安市莲湖区
10175	侯一百七十七	男	203	西安市碑林区	10176	侯一百七十八	女	197	西安市雁塔区
10177	侯一百七十九	男	205	西安市未央区	10178	侯一百八十	女	199	西安市新城区
10179	侯一百八十一	男	207	西安市灞桥区	10180	侯一百八十二	女	201	西安市莲湖区
10181	侯一百八十三	男	209	西安市碑林区	10182	侯一百八十四	女	203	西安市雁塔区
10183	侯一百八十五	男	211	西安市未央区	10184	侯一百八十六	女	205	西安市新城区
10185	侯一百八十七	男	213	西安市灞桥区	10186	侯一百八十八	女	207	西安市莲湖区
10187	侯一百八十九	男	215	西安市碑林区	10188	侯一百九十	女	209	西安市雁塔区
10189	侯一百九十一	男	217	西安市未央区	10190	侯一百九十二	女	211	西安市新城区
10191	侯一百九十三	男	219	西安市灞桥区	10192	侯一百九十四	女	213	西安市莲湖区
10193	侯一百九十五	男	221	西安市碑林区	10194	侯一百九十六	女	215	西安市雁塔区
10195	侯一百九十七	男	223	西安市未央区	10196	侯一百九十八	女	217	西安市新城区
10197	侯一百九十九	男	225	西安市灞桥区	10198	侯二百	女	219	西安市莲湖区
10199	侯二百零一	男	227	西安市碑林区	10200	侯二百零二	女	221	西安市雁塔区
10201	侯二百零三	男	229	西安市未央区	10202	侯二百零四	女	223	西安市新城区
10203	侯二百零五	男	231	西安市灞桥区	10204	侯二百零六	女	225	西安市莲湖区
10205	侯二百零七	男	233	西安市碑林区	10206	侯二百零八	女	227	西安市雁塔区
10207	侯二百零九	男	235	西安市未央区	10208	侯二百一十	女	229	西安市新城区
10209	侯二百一十一	男	237	西安市灞桥区	10210	侯二百一十二	女	231	西安市莲湖区
10211	侯二百一十三	男	239	西安市碑林区	10212	侯二百一十四	女	233	西安市雁塔区
10213	侯二百一十五	男	241	西安市未央区	10214	侯二百一十六	女	235	西安市新城区
10215	侯二百一十七	男	243	西安市灞桥区	10216	侯二百一十八	女	237	西安市莲湖区
10217	侯二百一十九	男	245	西安市碑林区	10218	侯二百二十	女	239	西安市雁塔区
10219	侯二百二十一	男	247	西安市未央区	10220	侯二百二十二	女	241	西安市新城区
10221	侯二百二十三	男	249	西安市灞桥区	10222	侯二百二十四	女	243	西安市莲湖区
10223	侯二百二十五	男	251	西安市碑林区	10224	侯二百二十六	女	245	西安市雁塔区
10225	侯二百二十七	男	253	西安市未央区	10226	侯二百二十八	女	247	西安市新城区
10227	侯二百二十九	男	255	西安市灞桥区	10228	侯二百三十	女	249	西安市莲湖区
10229	侯二百三十一	男	257	西安市碑林区	10230	侯二百三十二	女	251	西安市雁塔区
10231	侯二百三十三	男	259	西安市未央区	10232	侯二百三十四	女	253	西安市新城区
10233	侯二百三十五	男	261	西安市灞桥区	10234	侯二百三十六	女	255	西安市莲湖区
10235	侯二百三十七	男	263	西安市碑林区	10236	侯二百三十八	女	257	西安市雁塔区
10237	侯二百三十九	男	265	西安市未央区	10238	侯二百四十	女	259	西安市新城区
10239	侯二百四十一	男	267	西安市灞桥区	10240	侯二百四十二	女	261	西安市莲湖区
10241	侯二百四十三	男	269	西安市碑林区	10242	侯二百四十四	女	263	西安市雁塔区
10243	侯二百四十五	男	271	西安市未央区	10244	侯二百四十六	女	265	西安市新城区
10245	侯二百四十七	男	273	西安市灞桥区	10246	侯二百四十八	女	267	西安市莲湖区
10247	侯二百四十九	男	275	西安市碑林区	10248	侯二百五十	女	269	西安市雁塔区
10249	侯二百五十一	男	277						



**Figure 10. Natural image-caption pairs extracted by dots.ocr from diverse documents.** Our system effectively mines high-quality photographs and their corresponding descriptions from diverse document sources. These natural image-text pairs are crucial for enhancing the general visual understanding and cross-modal alignment capabilities of VLMs.

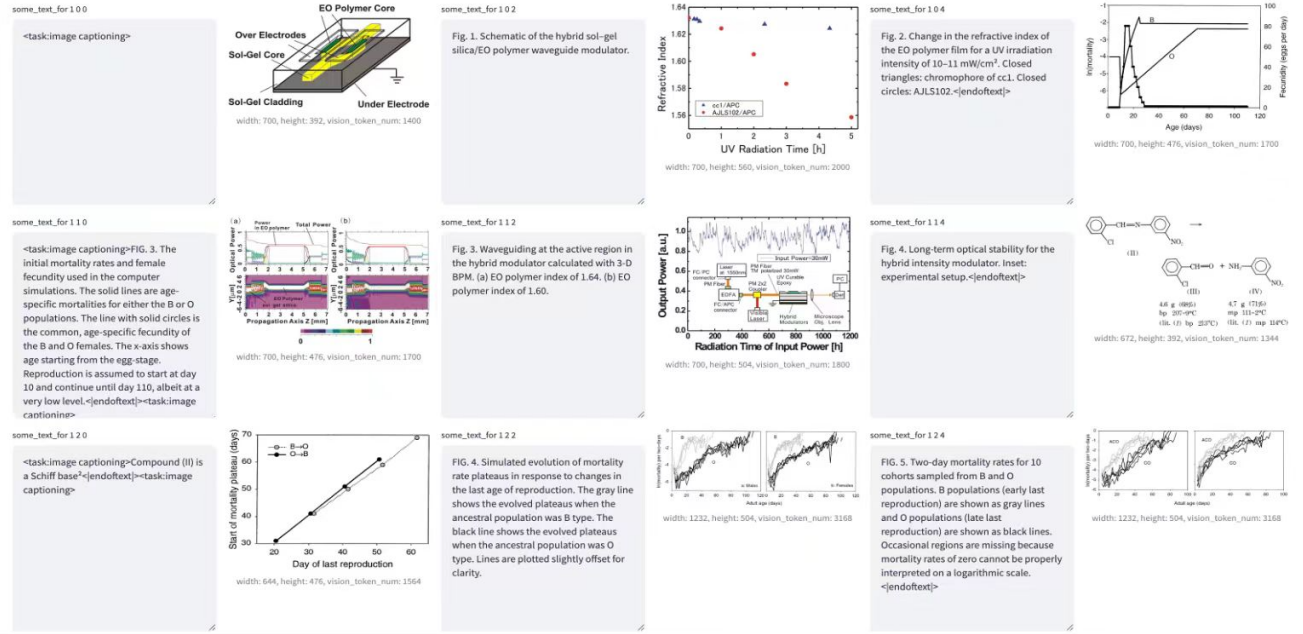


**Figure 11. Scientific figure-caption pairs extracted by dots.ocr.** Beyond natural images, our model accurately identifies and associates complex scientific charts, diagrams, and plots with their explanatory captions. This data is invaluable for training VLMs on domain-specific knowledge and fine-grained chart reasoning tasks.

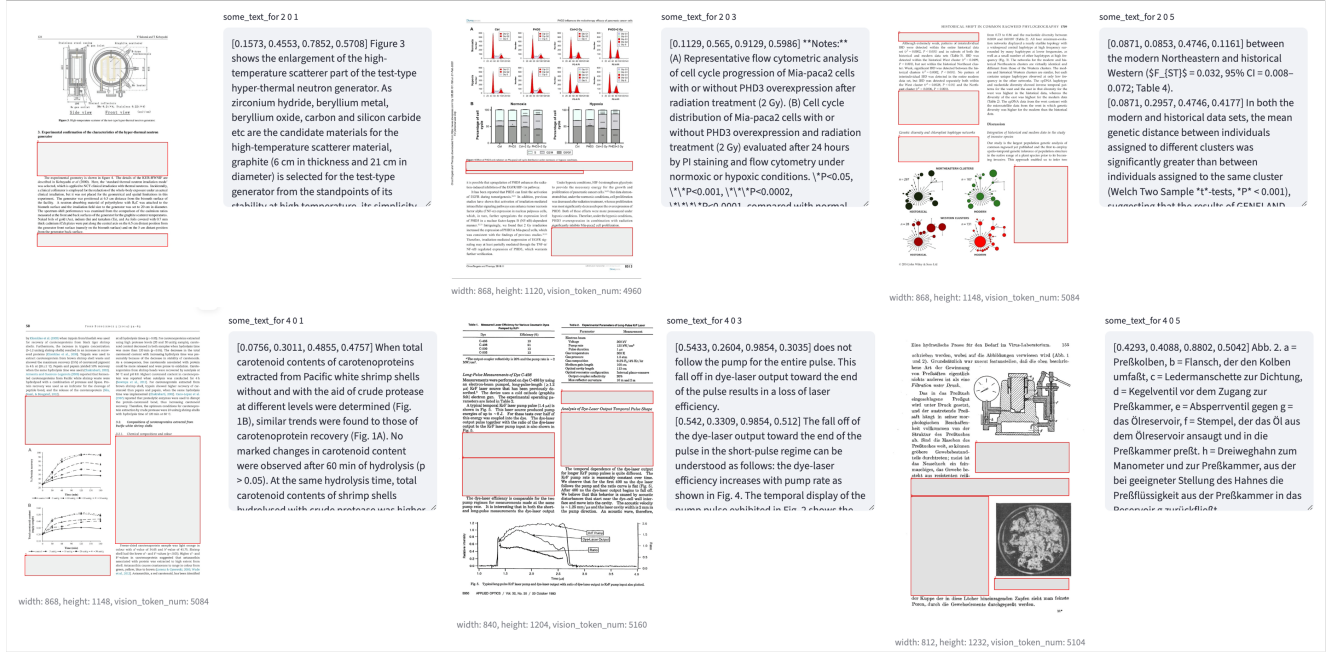


**Figure 12. Illustration of text-inpainting tasks generated with dots.ocr.** The system automatically masks text segments with precise bounding boxes, producing high-fidelity training data for models to predict missing content based on surrounding visual and textual context.



**Figure 13. Examples of next-page prediction pairs generated by dots.ocr.** For each current page, the corresponding next page is provided, allowing models to learn narrative flow and long-range document context.